



1 **Bacterial production in subarctic peatland lakes enriched by thawing permafrost**

2

3 Bethany N. Deshpande¹, Sophie Crevecoeur¹, Alex Matveev¹, and Warwick F. Vincent¹

4

5 ¹Centre for Northern Studies (CEN), Biology Department and Takuvik Joint International
6 Laboratory, Université Laval, Québec, QC, Canada

7 Running title: Bacterial production in thermokarst lakes

8 *Correspondence to:* B. N. Deshpande (bethany.deshpande.1@ulaval.ca)

9



Abstract. Peatlands extend over vast areas of the northern landscape. Within some of these areas, lakes and ponds are changing in size as a result of permafrost thawing and erosion, resulting in mobilisation of the carbon-rich peatland soils. Our aims in the present study were to characterize the particle, carbon and nutrient regime of a set of thermokarst (thaw) lakes and their adjacent peatland permafrost soils in a rapidly degrading landscape in subarctic Québec, Canada, and by way of fluorescence microscopy, flow cytometry, production measurements and an in situ enrichment experiment, determine the bacterial characteristics of these waters relative to other thaw lakes and rock-basin lakes in the region. The soil active layer in a degrading palsa (peatland permafrost mound) adjacent to one of the lakes contained an elevated carbon content (51% of dry weight), low C:N ratios (17:1 by mass), and large stocks of other elements including N (3% of dry weight), Fe (0.6%), S (0.5%), Ca (0.5%) and P (0.05%). Two permafrost cores were obtained to a depth of 2.77 m in the palsa, and CT scans of the cores confirmed that they contained high concentrations (>80%) of ice. Upon thawing, the cores released nitrate and dissolved organic carbon (from all core depths sampled), and soluble reactive phosphorus (from bottom depths), at concentrations well above those in the adjacent lake waters. The active layer soil showed a range of particle sizes with a peak at 229 μm , and this was similar to the distribution of particles in the upper permafrost cores. The particle spectrum for the lake water overlapped with those for the soil, but extended to larger (surface water) or finer (bottom water) particles. On average, more than 50% of the bacterial cells and bacterial production was associated with particles >3 μm . This relatively low contribution of free-living cells (operationally defined as the <1 μm fraction) to bacterial production was a general feature of all of the northern lakes sampled, including other thaw lakes and shallow rock-basin lakes (average \pm SE of $25 \pm 6\%$). However, a distinguishing feature of the peatland thaw lakes was significantly higher bacterial specific growth rates, which



33 averaged 4 to 7 times higher values than in the other lake types. The in situ enrichment
34 experiment showed no difference between organic carbon or phosphorus enrichment
35 treatments at day 5 relative to the control, however there was a significant, >100% increase in
36 bacterial growth rates between days 1 and 5 in the soil and the carbon plus phosphorus
37 enrichments. Collectively these results indicate that particles, nutrients and carbon are released by
38 degrading permafrost peatland soils into their associated thermokarst lakes, creating favorable
39 conditions for production by particle-based as well as free-living aquatic bacterial communities.
40 The reduced bacterial concentrations despite high cellular growth rates imply that there is strong
41 control of their population size by loss-related factors such as grazing and viral lysis.

42

43 Keywords: bacteria, climate change, northern lakes, peatlands, permafrost, thermokarst

44



45 **1 Introduction**

46 Aquatic environments in permafrost landscapes are biogeochemical hotspots that provide
47 microbial communities with access to substrates that have been previously locked in frozen soils
48 for centuries to millennia (Kling et al., 1991; Vonk et al., 2015). The highest soil organic carbon
49 contents of the permafrost environment are found in areas of sporadic or isolated permafrost
50 peatland, which span more than 5×10^5 km² of land in the circumpolar North (Tarnocai et al.,
51 2009). The availability of organic substrates from these vast permafrost peatland environments to
52 bacterial communities in aquatic ecosystems is likely to be influenced by a variety of factors,
53 including the soil biogeochemical composition, particle and molecular size, and potentially other
54 environmental factors, such as nutrient concentrations and temperature. Lakes in the boreal zone
55 with flat catchments dominated by forest and peatland areas are strongly heterotrophic systems
56 that have high rates of bacterial production (e.g., Kankaala et al., 2006), but less is known about
57 the bacterial characteristics of peatland lakes further northwards, in permafrost regions.

58 Decomposition processes in aquatic ecosystems are mediated by bacterial communities
59 that can be separated into two ecological groups: (1) free-living bacteria, in which solitary cells
60 are suspended in the medium and break down dissolved organic matter, and (2) particle-attached
61 bacteria, in which the communities are associated with various size-fractions of particles and
62 break down this particulate organic material, as well as accessing dissolved materials (Kirchman
63 and Mitchell, 1982). In both cases, these activities result in consumption of oxygen, production of
64 carbon dioxide, and the mineralization of organic materials.

65 In most lake and ocean environments, free-living bacteria dominate the total bacterial
66 community in terms of numerical abundance (Unanue et al., 1992; Kirchman and Mitchell, 1982;
67 Simon et al., 1990; Lami et al., 2009). However, there are many environments in which particle-



68 based bacteria play a major role. Several studies from estuarine- and marine-waters show that
69 particle-attached populations can account for 10 to 100 times more bacterial cells and activity
70 than free-living bacteria, depending on particle concentrations (Crump et al., 1999; Ghiglione et
71 al., 2007; Acinas et al., 1999; Lami et al., 2009). A study of seven freshwater ecosystems
72 including two marsh-systems showed that a small proportion of particle-attached bacteria (<10%)
73 was associated with >40% of the bacterial community activity, and it was hypothesized that lake
74 size may influence the presence of particulate matter for colonization via interactions between
75 sediments and the water column (Kirchman and Mitchell, 1982). In the turbid waters of the
76 Mackenzie River, which are strongly influenced by permafrost as well as fluvial erosion, more
77 than 90% of the total bacterial production was associated with particles >3 μm (Vallières et al.,
78 2008). Similarly, in the coastal waters of the Beaufort Sea, the >3 μm size-fraction often
79 accounted for >50% of total bacterial production (Garneau et al., 2006; Galand et al., 2008).
80 Other research has identified that a dominant portion (>50%) of bacterial cells were attached to
81 particles (Masin et al., 2012), especially in turbid systems with high concentrations of particulate
82 organic matter (Fletcher 1990; Lami et al., 2009).

83 Particle localisation of microbial processes has wide-ranging implications for trophic
84 processes in the water column and material fluxes to the sediments. In the oceanographic
85 literature, large particles are referred to as “marine snow”, and many studies that have shown the
86 importance of these aggregates for food-web dynamics (Michaels and Silver, 1988; Alldredge
87 and Silver, 1988; Kiørboe, 2001). Similarly, there has been attention given to “lake snow”;
88 Grossart and Simon (1993) found lake particle aggregates to be densely colonized by bacteria,
89 with approximately 10^8 bacterial cells per mL, 100 times higher than concentrations in the bulk
90 water. The presence of particle-attached bacteria may also result in greater community diversity,



91 as has been demonstrated in studies of estuarine mixing zones (Crump et al., 1998; Waidner and
92 Kirchman, 2007). A study by Ploug and Grossart (2000) identified a positive correlation between
93 bacterial production, particulate organic carbon and aggregate size. Size also affects sinking
94 velocities through Stokes' Law, and therefore the flux rates for transfer of materials from the
95 pelagic zone to the sediments (Ploug and Grossart, 2000).

96 Permafrost thaw lakes are rich in suspended particulate material as a result of permafrost
97 erosion (Breton et al., 2009; Watanabe et al., 2011). They are also continuously supplied with
98 organic as well as inorganic inputs from the thermokarst processes in their surrounding
99 catchments (Vonk et al., 2015), and there is increasing attention to the bacterial responses to such
100 inputs. In the Mackenzie River Delta region, a mesocosm assay showed decreased planktonic
101 bacterial production rates in response to permafrost soil enrichment, but a strong increase in
102 benthic bacterial production rates (Moquin and Wrona, 2014). In a set of subarctic thermokarst
103 ponds, late winter bacterial production was low and dominated by free-living bacterioplankton,
104 while much higher production rates in summer were dominated by particle-attached bacteria,
105 correlated with terrestrial carbon concentrations (Roiha et al., 2015). Permafrost peatland lakes
106 are known to be strong emitters of greenhouse gases with diverse microbiota (Liebner et al.,
107 2015), but little is known about the controls on their bacterial populations and productivity.

108 Our aims in the present study were to determine the distribution of bacterial production
109 between the suspended and free-living size fractions in subarctic peatland lakes, and their
110 responses to permafrost soil inputs. Two hypotheses were evaluated: firstly, that particle-attached
111 bacteria account for the dominant (>50%) fraction of the total microbial activity, and secondly
112 that organic carbon and nutrients originating from the erosion of permafrost soils promote
113 bacterial metabolic activity and cellular growth. We focused this research on a set of peatland



lakes in subarctic Québec and first determined the chemical composition of the soil active layer and underlying permafrost in a palsa (organic permafrost mound) that was adjacent to and eroding into a one of the peatland thaw lakes. We examined the distribution of soil particle sizes and compared these with particle distributions in lakes, with comparisons of particle size spectra, nutrients and organic carbon with other types of lakes in the region. We then measured bacterial abundance (BA) and production rates (BP) associated with different size fractions in the peatland and other lakes, and tested the effects of phosphorus, carbon and soil enrichment on bacterial concentrations and activity by way of an in situ incubation experiment.

2 Materials and methods

2.1 Study sites

The primary sampling sites were near Kuujjuarapik-Whapmagoostui (K-W, 55° 17' N, 77° 47' W) in thermokarst lakes and their surrounding soils in the peatland palsa valley of the Sasapimakwananistikw River (SAS; Fig. 1). Additional sampling for comparison took place in thermokarst lakes in the mineral lithalsa (mineral permafrost mounds) valley of the Kwakwatanikapistikw River (KWK) near K-W; glaciated rock-basin lakes, also near K-W, but not influenced by permafrost (RBL); and lithalsa lakes up to 200 km further to the North (SEC, BGR, NAS). This coastal region of northern Québec has experienced rapid climate change, including an increase in mean annual temperatures from -4.2 °C for 1932–1960 to $-2.6 \pm 1.2^{\circ}\text{C}$ for 2001–2010, accompanied by changes in the permafrost landscapes, including expansion of the tree line, changes to snow conditions, and various changes in thermokarst lakes frequency and extent (Bhiry et al., 2011). A total of 15 lakes were sampled at the five sites (Fig. 1; detailed location and depth information is given in Table S1 in the Supplement).



136 The SAS valley is an area of sporadic permafrost (<2% frozen ground) mainly colonized
 137 by *Sphagnum* and *Carex*, with dark brown and black colored thermokarst lakes (Arlen-Pouliot
 138 and Bhiry, 2005; Fillion et al., 2014). This peat bog contains more than 50 isolated permafrost
 139 mounds (palsas; Fig. 2) covered by a 60 cm soil active layer (Arlen-Pouliot and Bhiry, 2005;
 140 Fillion et al., 2014). Two sets of lakes were sampled in the SAS valley: SAS1 to the south and
 141 SAS2 located to the north of the river. The SAS lakes are stratified, heterotrophic lakes with
 142 anoxic zones throughout the majority of the water column, and surface waters that are under-
 143 saturated in oxygen (Deshpande et al., 2015). These lakes have abundant and active
 144 methanotrophic bacterial communities indicating their high methane supply rates (Crevecoeur et
 145 al., 2015), and they , emit greenhouse gases to the atmosphere at flux rates up to 10 mmol CH₄ m⁻²
 146 d⁻¹ and >200 mmol CO₂ m⁻² d⁻¹ (A. Matveev et al., unpublished).

147 The valley of the Kwakwatanikapistikw River (KWK) is also in an area of sporadic
 148 permafrost, located only 8 km from SAS. It is colonized by lichen-moss, shrub-tundra vegetation,
 149 and forest patches in wind-sheltered areas (Arlen-Pouliot and Bhiry, 2005), and contains
 150 numerous thermokarst lakes that vary in color from blue-green to brown. The SEC site (55°
 151 42.067' N, 76° 38.604' W) was located 86.0 km north-east of K-W and the BGR site was located
 152 near the Hudson Bay and the village of Umijuaq (56° 36.63' N, 76° 12.85' W), both in areas of
 153 discontinuous permafrost. BGR1 appears to be a rapidly expanding lake, with a maximum depth
 154 of 3.2 in 2006 (Breton et al., 2009) that had increased to 4.0 m in 2013 (Deshpande et al., 2015),
 155 and 4.2 m in the present study. The Nastapoka River valley (NAS) contains thermokarst lakes
 156 that were formed by thawing lithalsa mounds in this region of continuous permafrost. The non-
 157 permafrost-affected, rock-basin lakes (RBL) in the K-W region are of similar area and shallow



158 depth (0.8 – 2.1 m) to the thermokarst systems, but with rock substrate catchments rather than
 159 permafrost soils.

160 **2.2 Lake sampling and profiling**

161 Sampling took place during three consecutive summers from 2012 to 2014. At each visit, surface
 162 water was sampled using sterile plastic containers. A Van Dorn sampler was used to retrieve
 163 samples from the oxycline or the bottom waters, 0.2 above the bottom sediments. Water samples
 164 were analysed for soluble reactive phosphorus (SRP), total nitrogen (TN), dissolved organic
 165 carbon (DOC), Chlorophyll *a* (Chl *a*), and total suspended solids (TSS) according to methods in
 166 Laurion et al., (2010). Ammonium and nitrate (including nitrite) concentrations were measured in
 167 water from the SAS valley only using a Lachat autoanalyzer (detection limit of 10 µg N). Soil
 168 was sampled from the active layer directly next to a lake at each site and stored in sterile plastic
 169 bags. Frozen samples of both water and soils were returned to Université Laval (Laboratoire de
 170 géomorphologie et de sédimentologie, FFGG) to determine particle size distribution via Laser
 171 Particle Size Analyzer (LA-950V2, Horiba Ltd., Japan).

172 For CDOM analysis, water samples from the surface waters of the SAS lakes were filtered
 173 through sample-rinsed 0.47 mm, 0.2 µm pore size cellulose acetate membrane filters and the
 174 filtrate was analyzed with the Varian Cary 100 UV-VIS spectrophotometer. The absorbance
 175 scans were obtained from the spectrophotometer over the wavelength range of 200-850 nm at
 176 natural pH using a 1-cm acid-cleaned quartz cuvette on dual beam mode, at a speed of 240 nm
 177 min⁻¹ with a slit width of 1 nm. The absorbance was measured against ultra-pure water and
 178 corrected against the blanks prepared on site. Absorption coefficients were calculated as $a(\lambda) =$
 179 $2.303 \times A(\lambda)/L$, where $a(\lambda)$ is the absorption coefficient at a wavelength λ , $A(\lambda)$ is the optical
 180 density (absorbance) for wavelength λ , and L is the path length of the cuvette (m). Spectral slope



parameters were also determined from absorbance at 275nm (a_{275}) and 295 nm (a_{295}) using the formula $a_{295} = a_{275}e^{-S(295-275)}$, where S (nm^{-1}) is the spectral slope parameter (Fichot and Benner, 2012).

2.3 Active layer and permafrost core sampling

Triplicate soil samples were retrieved from the surface active layer of a palsa adjacent to lake SAS1B on 3 August 2013; the soil was sampled from half way up the face of the palsa (approximately 1 m above the lake surface) that was eroding and collapsing into the lake (Fig. 2). Subsamples were frozen and transported to Quebec City for CHN (LECO analyzer, CEN, Québec) and other geochemical analyses (ICP-AES; INRS-ETE, Québec). Enrichment Factors (EF) for the soil samples were determined as per Gorham and Janssens (2005):

$$EF_{soil} = \frac{[x]_{sample}/[Al]_{sample}}{[x]_{soil}/[Al]_{soil}}$$

where $[x]_{sample}$ is the concentration of a given element, x , in the study sample, $[Al]_{sample}$ is the concentration of the element Al in the study sample, $[x]_{soil}$ is the world median concentration of element x , and $[Al]_{soil}$ is the world median concentration of the element Al. Global average values were taken from Bowen (1979).

Permafrost cores were sampled from two sites 15 m apart on large an organic-rich palsa mound at the SAS2 site (Fig. 1) on 5 August 2013 using a portable drill system (Calmels et al., 2005). The recovered cores were 10-cm in diameter, with lengths of 2.8 and 3.0 m. Samples were returned to the Centre for Northern Studies (Université Laval, Québec) and maintained frozen. The frozen core was characterized by CT scanning (Calmels and Allard, 2004) and later subsampled. Subsamples were 1.5-cm thick and centered at depths of 1.25, 1.75, and 2.77 m from each of the two permafrost cores. Each sub-sample was placed in a sterilized container filled with



202 ultrapure Milli-Q water and thawed for a period of 48-hours. Samples were then lightly shaken
 203 and then filtered through 0.47-mm, 0.2- μm pore size cellulose acetate membrane filter. The
 204 filtrate and a blank (Milli-Q water) were analysed for DOC, NO_3^- (including NO_2^-) and SRP
 205 (INRS-ETE, Québec). DOC was analyzed using a Shimadzu 5000A TOC Analyzer (detection
 206 limits of 0.05 mg C L^{-1}). SRP and NO_3^- were analyzed using a Lachat autoanalyzer (detection
 207 limit of 1 $\mu\text{g N}$ and P L^{-1}). CDOM was analyzed as described above. Unfiltered diluted samples
 208 were analyzed for particle-size distribution as described above. Additional subsamples from
 209 throughout the core were analysed for total CHN content (LECO analyzer, CEN).

210 **2.4 Size-fractionation**

211 Surface water was sampled from the pelagic zones of lakes BGR1, SEC, KWK12, SAS2A,
 212 NAS1A and RBL4K for size fractionation. Phytoplankton and particle-attached bacterial
 213 communities were filtered through a 35- μm Nitex screen. The bacteria were then further
 214 separated into two size fractions: either by passing through a glass fibre filter (Pall Canada Ltd.)
 215 with a nominal pore size of 3.0 μm , or by further filtration through a Whatman GF/B glass fibre
 216 filter with a nominal pore size of 1.0 μm . Approximately 2.0 L was filtered for each size fraction,
 217 and an unfiltered total community sample was also preserved for concurrent analysis.

218 **2.5 Bacterial community counts**

219 The bacterial communities in the size-fractionated samples were counted after staining with 4',6-
 220 diamidino-2-phenylindole (DAPI). Samples were preserved with formaldehyde (3.7% final
 221 concentration) in pre-washed plastic bottles, pre-rinsed with the sample and stored at 4°C for up
 222 to 6 months. Samples were later shaken to break up larger particles and then filtered onto
 223 Nuclepore black polycarbonate membranes (0.22 μm , 25 mm) placed on cellulose acetate



backing filters (0.7 μm , 25 mm) under low pressure. DAPI was added to 1.5 mL of sample (4 μg mL⁻¹ final concentration) and left to stain for 10 min before filtering until dry. Filters were mounted on slides with coverslips and non-fluorescent immersion oil, and stored at -20°C until counting on a Zeiss Axioskop 2 epifluorescence microscope, under UV light and 1000 \times magnification with immersion oil. A minimum of 15 fields or 400 cells were counted of each sample triplicate.

All other bacterial samples were counted via flow cytometer (FACSCalibur, BD Biosciences Inc., USA) following the procedure described in Rossi et al. (2013). Samples were fixed with glutaraldehyde (1% final concentration) and stored at -80°C until analysis. Bacterial samples were then shaken and stained with the nucleic acid dye SYBR Green I (40 μL mL⁻¹ final concentration) for 10 min in the dark, and processed at a low flow rate (12 μL min⁻¹) using 1 μm yellow-green microspheres (Polysciences) solution as an internal standard. Bacterial cells were enumerated based on fluorescence (FL1) and side-scatter characteristics, with data analyzed using the CellQuest Pro software.

2.6 Bacterial production

Bacterial production rates were measured via protein synthesis using radio-labelled leucine incorporation (Kirchman, 2001). Triplicate microfuge tubes plus a killed control each containing 1.5 mL of sample and 40 nM of [4,5-³H]leucine (60 Ci mmol⁻¹, PerkinElmer Inc.) were incubated for 1 h at 15°C. After one hour, biomass production was halted by the addition of 100 μL of trichloroacetic acid (100%) and stored at 4°C. Later, the samples were returned to the Takuvik radio-isotope laboratory at Université Laval. Samples were processed using the centrifugation method of Smith and Azam (1992) and then radio-assayed in a scintillation counter to measure the ³H-leucine uptake. Net bacterial C production was estimated using a conversion factor of 3.1



kg C per mole of leucine (Kirchman et al., 1993; Iriberry et al., 1990). Bacterial community specific growth rates were determined using an average cellular carbon content of 18 fg C cell⁻¹, as measured in the nearby KWK lakes (Roiha et al., 2015).

2.7 Enrichment experiment

At lake SAS1B, the following treatments were added to triplicate 20 L containers of lake water: 43 μmol L⁻¹ of glucose (G; to achieve an estimated 20% increase of ambient DOC based on previous measurements), 1.8 μg L⁻¹ of phosphorus (P; 10% enrichment of total P), glucose and phosphorus together (G+P), and 6.2 mg L⁻¹ of an aqueous suspension of the soil from the SAS1B palsa face, sampled and analyzed as described above (S; equivalent to 20% increase in total carbon relative to ambient DOC). A sample control was also prepared (C). Samples were taken immediately after enrichment (t₀), and from each container after 5 days (t₅) of incubation in situ in the near-surface waters of SAS1B. Chl *a*, bacterial concentrations and bacterial production rates were measured in each treatment.

2.8 Statistical analysis

Environmental and bacterial variables for the comparison of lake waters were analysed by 1-way ANOVA. A 2-way ANOVA was used to compare environmental and biological differences between surface and bottom waters of the various lake types. For the size-fractionation data, a 2-way ANOVA was performed on pre-standardized variables, with the factors of lake and size-fraction following the Shapiro normality test. The enrichment experiment was analyzed via 2-factor repeated measures ANOVA, with each replicate individually tracked. Variables before and after enrichment were also compared via Holm-Sidak pairwise comparisons. Bacterial community growth rates were normalized by square root transformation, and bacterial



abundance was log transformed. Analyses were done using GraphPad Prism (v. 6.0f, GraphPad Software Inc., USA) and SigmaPlot (v. 12, Systat Software Inc., USA).

3 Results

3.1 Active layer soil analyses

The SAS active layer extended to 60 cm depth and contained 509 g kg⁻¹ of carbon, or 50.9% of the soil by mass, and 30 g kg⁻¹ of nitrogen (Table 1). Several elements were present in substantial concentrations, including phosphorus at a mean value (±SD) of 545 (19) mg kg⁻¹, iron at 6.0 (1.6) g kg⁻¹, and calcium at 5.2 (3.4) mg kg⁻¹. The soil enrichment factors (EF) were used to compare concentrations of soil elements with world medians (Bowen, 1979) to determine whether the elements were derived uniquely from wind-blown mineral soil (EF ≤ 1), or were more likely to accumulate due to multiple sources (EF >> 1) (Gorham and Janssens, 2005). Several elements had EF values < 1, including K, Na, and Mg. For Al, Mn, Pb, Cr, Zn, and Ba, the EF values were between 1 and 2. Phosphorus had an EF of 16, and S had the highest EF value of 132.

3.2 Permafrost core analysis and comparison with lakewater

The frozen permafrost cores were composed mainly of organic matter intercalated with ice (>80%) in the two upper levels, with high concentrations of sediment only in the deepest level at ~2.77 m (Table 2). The soils throughout the core released water containing nitrate and high concentrations of DOC, and the sediment-containing matter near the bottom of the cores additionally released SRP at concentrations up to 30 times those measured in the SAS lakes.

The $a_{CDOM}(\lambda)$ spectra for the DOC from the upper two permafrost core samples were almost identical, but differed greatly from those for the bottom-core samples (Fig. 4). Values of $a_{CDOM}(440)$ ranged from 9.96 to 16.2 m⁻¹ in all permafrost core samples except the bottom of core



291 A, which was 51.5 m^{-1} . The spectral slope parameter ($S_{275-295}$) ranged from 0.0087 to 0.014 nm^{-1}
 292 in the permafrost cores. For SAS lake water samples, $a_{\text{CDOM}}(\lambda)$ spectra were similar to those
 293 observed from the permafrost core samples (Fig. 4). $a_{\text{CDOM}}(440)$ ranged from 8.63 to 18.1 m^{-1} ,
 294 and was consistently higher in bottom waters than in surface. Spectral slope parameters ($S_{275-295}$)
 295 for the SAS water were within a notably smaller range than for the permafrost cores, and ranged
 296 from 0.011 to 0.012 nm^{-1} .

297 3.3 Particle size distribution in soils and lakes

298 The particle-size distributions from the SAS permafrost cores followed a bimodal distribution as
 299 observed in the SAS active layer soil and the SAS lake water (Fig. 5). The maximum frequency
 300 of particle size (PS_{max}) ranged from 152 to $200 \mu\text{m}$ for the permafrost layers at 1.25 and 1.75 m
 301 for both duplicates. The bottom layer of core A had a distribution maximum of $67 \mu\text{m}$ while the
 302 maximum for core B was $51 \mu\text{m}$. The active layer soil was similar to the distribution of particles
 303 in the upper permafrost cores, but with a maximum frequency at a slightly higher size ($229 \mu\text{m}$),
 304 and an even distribution of particles from 80 to $300 \mu\text{m}$. The particle spectrum for the SAS lake
 305 water overlapped with those for the soil, but the surface water spectrum extended to higher sizes
 306 and peaked at $394 \mu\text{m}$, while the bottom water spectrum peaked at $200 \mu\text{m}$ and extended to finer
 307 particles (Fig 5).

308 As a further analysis of particle size distribution, difference spectra were calculated
 309 relative to the SAS2A surface waters for the active layer soil, upper permafrost soil and bottom
 310 waters. These curves emphasize the strong overlap in size spectra, with differences ranging from
 311 only -3 to $+6\%$, depending on size class (Fig. 6). These curves also illustrate how the surface
 312 water was slightly enriched in larger particles, while the bottom waters were enriched in finer
 313 particles.



314 Within-lake particle sizes showed highly variable distributions across the other lakes
 315 studied, with modes that ranged from 4 to 1337 μm (Table 3; Fig. 5). The smallest particles were
 316 identified in RBL4K, a rock-basin lake unaffected by permafrost, with a mode particle size of 4
 317 μm . Of the thaw lakes, the lakes from areas of sporadic, degrading permafrost had larger particles
 318 than the continuous- and discontinuous-permafrost lakes. For example, the mode particle sizes in
 319 NAS1A, BGR1, and SEC were 102, 59, and 153 μm , respectively. In contrast, the particle-size
 320 modes in SAS2A and KWK12 were 300 μm and 592 μm , respectively.

321 The concordance of particle distributions between the lake waters and their adjacent soils
 322 varied among the other sample sites (Fig. 5). For example, the distribution of particles in KWK12
 323 was strikingly similar to that of KWK active layer soil, while other lake samples tended to have
 324 modes that were higher than the mode observed in the soil, as in SAS. For example, the mode for
 325 BGR lake water was 59 μm , but 10 μm for the adjacent mineral soil. As at SAS, the distribution
 326 of soil and lake water particles at SEC was bimodal, and the particles encompassed a much wider
 327 range in soil than in the lakes.

328 **3.4 Lake properties**

329 The SAS lake surface waters differed significantly in their limnological properties from those of
 330 other thaw lakes and also from the rock-basin lakes (Table 3; 1-way ANOVA). The SAS lakes
 331 had a mean surface DOC value of 11.5 mg L^{-1} , that was significantly higher than the two other
 332 lake categories (Mann-Whitney test, $p = 0.004$). The average surface Chl *a* concentration of 2.29
 333 $\mu\text{g L}^{-1}$ was also significantly higher for the SAS lakes relative to the other categories ($p = 0.03$),
 334 as was surface TN, which averaged 0.58 mg L^{-1} ($p = 0.004$). TSS and maximum particle size
 335 (PSmax) values were variable within each lake type (Table 3), with no significant differences; the
 336 surface PSmax values were strikingly variable in rock-basin lakes, ranging over three orders of



337 magnitude, but much more homogeneous among the SAS waters (mean of 384 μm with a CV of
 338 37%).

339 The SAS lakes were well stratified and despite their shallow depths showed substantial
 340 differences between the top and bottom of the water column, which was also a feature of the
 341 other thaw lakes (Table 3). A two-way ANOVA for depth and the two thaw lake types (SAS
 342 versus the other thaw lakes) showed that overall there were significant increases at depth in SRP
 343 ($F = 23$; $p = 0.03$); TN ($F = 18$; $p = 0.02$) and Chl *a* ($F = 28$; $p = 0.03$), with no significant ($p >$
 344 0.05) top-bottom differences in DOC, TSS or PSmax. Consistent with the 1-way analysis for all
 345 three lake types, this 2-way analysis (both depths) showed that SAS lakes had significantly
 346 higher concentrations of DOC ($F = 65$; $p < 0.0001$) and TN ($F = 32$; $p = 0.004$) relative to other
 347 thaw lakes. However, the SAS lakes had significantly lower concentrations of TSS ($F = 23$; $p =$
 348 0.05), which were especially high in NAS1A and BGR2, and there were no significant
 349 differences ($p > 0.05$) between the two groups of thaw lakes in terms of SRP, Chl *a* or PSmax.

350 Ammonium and nitrate were not analyzed routinely, but the surface waters of the SAS
 351 lakes sampled during late June 2014 contained undetectable concentrations of nitrate ($<10 \mu\text{g N}$
 352 L^{-1}) and substantial concentrations of ammonium: 64 (SAS1A), 58 (SAS1B), 49 (SAS2A), 60
 353 (SAS2B) and 74 (SAS2C) $\mu\text{g NH}_4^+\text{-N L}^{-1}$. Much higher values were recorded in the anoxic
 354 bottom waters of two of the lakes: 1021 (SAS1A) and 178 (SAS1B) $\mu\text{g NH}_4^+\text{-N L}^{-1}$, but values
 355 were similar to surface waters in SAS2A (48 $\mu\text{g NH}_4^+\text{-N L}^{-1}$).

356 **3.5 Bacterial abundance and productivity**

357 Bacterial abundance in the surface waters varied over an order of magnitude among SAS lakes,
 358 from 2.0×10^5 to 3.1×10^6 cells mL^{-1} , and did not significantly differ from the other lake types



(Table 4; $p > 0.05$). Bacterial production rates varied by a factor of six among SAS lakes, from 0.25 to $1.68 \mu\text{g C L}^{-1} \text{ h}^{-1}$, and as for cell concentration, there were no significant differences among the categories of lakes. Bacterial cellular growth rates were similarly variable, ranging from 1.9 to $113 \text{ fg cell}^{-1} \text{ d}^{-1}$, however four of the five surface values were well above (factor of two or greater) any of the lakes in the two other lake categories, and the mean value for SAS waters was significantly higher than the others ($F = 5.0$; $p = 0.026$).

3.6 Size-fractionated solids and associated bacteria

In SAS2A, the mass of suspended solids decreased sharply with filter size, and the $<1 \mu\text{m}$ fraction contained only 5% of the total value (Fig. 7). Similar trends were observed in the other lakes, with the exception of NAS1A where almost all of the suspended solids passed through the 35 and $3 \mu\text{m}$ filters, and 34% even passed through the $1 \mu\text{m}$ filter. In terms of bacterial cells, highest counts were in the total or $<35 \mu\text{m}$ fraction, with the exception of NAS1A, which peaked in the $<3 \mu\text{m}$ fraction. Only 28% of the maximum counts occurred in the $<1 \mu\text{m}$ fraction in SAS2A samples, and this fraction was similarly low in SEC (23%). Higher percentages of maximum occurred in the $<1 \mu\text{m}$ fraction in RBL4K (43%), KWK12 (52%), BGR1 (52%) and NAS1A (87%).

The bacterial production data showed a more striking pattern (Fig. 7). Total production was maximal in the unfiltered (total) or $<35 \mu\text{m}$ fraction, but the $<1 \mu\text{m}$ fraction accounted for only 26% of the maximum in SAS2A, and was even lower in most of the other lakes: 11% (NAS1A), 11% (RBL4K), 16% (KWK12), and 14% (BGR1). An average value of 39% was recorded in SEC. The cellular growth rates (BG) were highly variable among size fractions (Fig. 6). In the SAS2A analysis, rates were two times higher in the $<3 \mu\text{m}$ than in the $<1 \mu\text{m}$ fraction. Similarly, in all of the other lake waters, highest cellular growth rates were in fractions above $1 \mu\text{m}$: Total



(NAS1A); Total and $<3 \mu\text{m}$ (BGR1); $<3 \mu\text{m}$ (SEC); Total (KWK12) and Total and $<35 \mu\text{m}$ (RBL4K). The free-living cell fraction ($<1 \mu\text{m}$) showed rates that were a small percentage of the production per cell in the unfiltered samples in RBL4K (27%); KWK12 (16%); NAS1A (8%) and BGR1 (16%).

3.7 Enrichment experiment

Over the course of the experiment (Fig. 8), there was no significant change in Chl *a* concentrations, either with time or among treatments (repeated measures ANOVA, $p > 0.05$). There was a significant drop in cell abundance in all treatments by day 5 (BA; effect of time $F = 39$; $p = 0.025$) but no significant change in production rates (BP, $p > 0.05$). Although there was no significant overall effect of time and treatment on bacterial growth rates (BG, carbon production rates per cell; $p > 0.05$), there was a significant interaction effect between time and treatment ($F = 4.9$; $p = 0.026$). Further analysis (Holm-Sidak pairwise comparisons) showed that while most of bacterial growth rates had not changed statistically, there was a large significant increase between days 1 and 5 in the soil addition treatment (146% average increase; $t = 2.9$; $p = 0.034$) and in the carbon+phosphorus (G+P) enrichment (187% increase; $t = 3.34$; $p = 0.022$).

4 Discussion

4.1 Organic carbon enrichment

There is an estimated $1.048 \times 10^6 \text{ km}^2$ of permafrost peatland in North America, half of which is located in areas of sporadic or isolated permafrost like the SAS region of the present study (Tarnocai et al., 2009). The surface soil and permafrost cores from the SAS region were abundant in carbon, with $\sim 50\%$ C-content (by dry-weight) down to 2 m depth in the permafrost cores (Fig. 3). These values are comparable to peatland soils elsewhere. A study of peat cores from five



404 North-American sites showed that the concentration was consistently around 50% C dry-weight
 405 (Gorham and Janssens, 2005), as was also observed in the surface SAS1 active layer and in the
 406 upper layers of the two permafrost cores. Similarly, a synthesis of peat data from 9 studies in the
 407 northern hemisphere (Gorham et al., 2012) yielded a mean value (\pm SD) of 50.1 (2.9). These
 408 carbon values are much higher than observed in other types of Arctic soils. For example, the
 409 carbon content of active layer soil from a polygonal tundra of the Lena Delta ranged from 1.5 to
 410 3% dry-weight (Höfle et al., 2013), an order-of-magnitude less than values in the SAS soil.
 411 Lower carbon concentrations were also measured in a study of permafrost soils of the Arctic
 412 tundra of Northwest Territories, which were 6.5% C (Moquin and Wrona, 2015), and in the
 413 lithalsa mounds surrounding BGR1 (Fig. 1), where the carbon content of the active layer was less
 414 than 1% (ADAPT, 2014).

415 Paleocological studies (Arlen-Pouliot and Bhiry, 2005; Fillion et al., 2014) have shown
 416 that the peat in the SAS valley accumulated in bogs over a 1400 year period from around 1800 to
 417 400 years before the present, and was then uplifted in palsas during the period of permafrost
 418 aggradation during the Little Ice Age, 400 to 200 years before present day. From the end of the
 419 19th century onwards, the SAS palsas have been thawing and eroding, with the production and
 420 eventual infilling of associated thermokarst lakes (palsa lakes), and this warming phase appears
 421 to have accelerated over the last two decades (Bhiry et al., 2011). The degrading palsas are
 422 therefore a rich source of organic carbon to their associated lakes. As shown in the permafrost
 423 core analysis (Table 2), this organic input includes not only particulate organic carbon but also
 424 DOC. Two contrasting scenarios have been identified for the effects of thawing permafrost on
 425 carbon transport in northern catchments (Vonk et al., 2015): (1) decreased net export of carbon as
 426 a result of increased flow path lengths, residence times and decomposition in a deeper active



layer, or (2) increased net export as a result of thermal erosion and mobilisation of particulate and dissolved organic carbon. The SAS valley is currently in the ‘pulse phase’ of carbon mobilisation, which as noted by Vonk et al. (2015), is typically dominated by the export of particulate materials. However, the high DOC of the SAS waters, significantly above that in the other lake types, also attests to a substantial export of DOC from the SAS palsas to their associated lakes, and is consistent with the permafrost thaw analyses. The low spectral slope values in the SAS lakes indicate a predominantly terrestrial origin of DOC in these lakes (Fichot and Benner, 2012), and the similarity in slope values between the permafrost cores and the lake waters also supports this close linkage between land and water.

4.2 Nutrient enrichment

The SAS soil likely represents a nutrient-rich substrate for bacterial metabolic activity. The soil N concentrations were low relative to C, reflecting the stoichiometry of ancient moss tissue, however there were large standing stocks of this element, and the high ammonium levels in the lake water implies that nitrogen was in abundant supply for planktonic microbial growth processes. The SAS surface soil had nearly three times as much phosphorus and more than five times as much iron relative to concentrations found in other *Sphagnum* peat bogs (Gorham and Janssens, 2005). It had 1.6 times the concentration of phosphorus and three times the amount of calcium when compared to permafrost soil from the Northwest Territories (Moquin and Wrona, 2015), though only a fraction (5%) of the magnesium observed in the latter study. Enrichment Factors (EF) indicated that phosphorus was above the global average for phosphorus concentrations in soil (EF=15.9), demonstrating long-term transfer of this elements from other sources, such as via atmospheric deposition or hydrological transfer. The permafrost thawing analyses showed a release of nitrate but no evidence of soluble phosphorus release, except from



the bottom-core samples that produced SRP concentrations that were 2- to 30-times above current lake water values. This coastal region of eastern Hudson Bay was submerged beneath the Tyrell Sea from immediately after the retreat of the ice cap about 7900 years ago to emersion from the sea about 6000 years before the present, and previous paleoecological studies on the deeper strata of the SAS valley sampled in the bottom core show that these are ancient marine sediments (Arlen-Pouliot and Bhiry, 2005; Fillion et al., 2014). This would account for their higher phosphorus release relative to that from the upper core. Deep thawing of the palsas during the final stages of their collapse could therefore have a major P-enrichment effect on the associated thermokarst lake ecosystems.

Inorganic nutrient release from thawing and eroding permafrost has been documented at sites elsewhere, but with large variations among regions and landscape types (Vonk et al., 2015). Slumping of permafrost soils into Alaskan streams increases their inorganic as well as organic concentrations (Bowden et al., 2008), but phosphorus adsorption onto clays may decrease SRP concentrations in some mineral permafrost environments (Breton et al., 2009). Nitrate export from the Kuparuk River catchment on the Alaska North Slope increased 5-fold between the late 1970s and early 2000s and may have been related to permafrost soil and vegetation effects (McClelland et al., 2007).

4.3 Particle enrichment

The permafrost peatland lakes were rich in particulate material, with substantially larger particles than non-permafrost-affected rock-basin lake RBL4K, and they contained some of the largest particles amongst thermokarst lakes studied (Fig. 5). Much finer particles over a narrower size range were recorded in the northern permafrost lakes NAS1A and BGR1, reflecting their mineral permafrost catchments. The close correspondence between the active layer, permafrost and lake



473 particle size distribution at SAS2 (Fig. 6), is evidence that this richness of particles in the
474 peatland lakes is derived from the thermo-erosion of their associated palsas. The small but
475 conspicuous shift to larger particles in the SAS surface waters may indicate the production of
476 aggregates by flocculation that are maintained in the upper water column by virtue of their low
477 density and therefore slow sinking speeds. The production of flocs was observed when SAS
478 water was brought into the laboratory and stored in clear glass bottles without mixing for several
479 days (B. N. Deshpande, unpublished observations), and may be favored by the high DOC
480 concentration in these waters. In contrast, the deeper waters showed an increase in fine particles,
481 contrary to what might be expected from Stokes' Law based upon size relationships. The origin
482 of this difference is unknown at this time, but it could be the result of fine, high-density mineral
483 particles settling out from the overlying water column. The extreme thermal stratification and
484 physical stability of these waters (Deshpande et al., 2015; Przytulska et al., 2016) indicates that
485 only particles of small size or low density would be maintained in the water column.

486 **4.4 Bacterial association with particles**

487 There was clear evidence that the high particle-loading of SAS waters affected its bacterial
488 ecology. Less 30% of the total cells and productivity were associated with the free-living
489 category, operationally defined here as passing through a 1 μm filter, and this effect was even
490 more pronounced for bacterial growth rates, which were 50% lower in the $<1 \mu\text{m}$ than in the <3
491 μm fraction, implying much faster growth rates of bacteria on particles in the size range 1-3 μm .
492 In SAS2A, as in many of the other northern lakes, bacterial populations and production appeared
493 to be distributed across the full range of particle sizes. This is consistent with studies across a
494 range of salt- and fresh-water environments showing that particle-attached bacteria are favored in



495 environments with a high availability of particulate habitats (Lami et al., 2009; Kirchman and
496 Ducklow, 1987; Kirchman and Mitchell, 1982).

497 There are several sources of experimental error that must be considered when interpreting
498 particle analyses of this sort. Firstly, it is difficult to obtain a reliable count of particle-based
499 bacteria. Our shaking of the samples would have broken up and released cells from larger
500 aggregates, but dislodging bacteria from particles is notoriously difficult. Even sonication is not
501 completely effective, and addition of a detergent along with sonication can result in a
502 pronounced increase in cell concentrations in sediment-laden waters (Yoon and Rosson, 1990). It
503 is therefore likely that the cell concentrations in the present study were underestimated, especially
504 in the $>1\ \mu\text{m}$ fractions. This would imply an even greater representation by particle-based cells to
505 the total community abundance, but it would also have led to an overestimation of the production
506 rates per cell biomass. Experiments based on size-fractionation by filtering are always
507 challenging because of the interactions between particle and the filters. Filtering water results in
508 the breakup of particles upon collision with the filter surface, causing two important effects: (1)
509 an increased bioavailability of organic particles (Amon and Brenner, 1996); and (2) potential
510 detachment of particle-attached bacterial from their organic-matter habitat. Filter blocking may
511 have also retained smaller fractions, including free-living cells. Although the exact rates per
512 fraction in the present study, as in all such studies, must be interpreted with caution, the
513 distribution of cells and activities across multiple fractions and the low values in the $<1\ \mu\text{m}$
514 fraction point to the importance of particle-based bacteria in this system. This was not unique to
515 SAS waters, but was found in several of the other lakes. These results are consistent with a
516 previous study of five lakes in the KWK area, which showed a substantially higher proportion of
517 particle-attached bacteria ($62\pm 30\%$ in the $>3\ \mu\text{m}$ size-fraction) and high productivity ($59 \pm 30\%$)



by these groups (Roiha et al., 2015). The production-per-cell patterns are also consistent with data elsewhere; for example, Kirchman and Mitchell (1982) found that particle-attached bacteria accounted for <10% of the total bacterial populations but contributed substantially to total microbial activity.

4.5 Controls on bacterial abundance and productivity

Bacterial abundance in the thermokarst lakes sampled here ranged from 0.20 to 3.5×10^6 cells mL^{-1} , which falls towards the higher end of the range for comparable aquatic ecosystems (Table 5). For example, in study of 16 lakes located in subarctic Sweden, bacterial concentrations ranged from 0.4 to 2.4×10^6 cells mL^{-1} (Karlsson et al., 2001), and in a humic, boreal lake, bacterial concentrations ranged from 1.2 to 1.7×10^6 cells mL^{-1} in winter (Tulonen et al., 1994).

The bacterial production rates in the thermokarst lakes sampled here were also at the high end of the range in comparable systems (Table 5), from 0.25 to $2.3 \mu\text{g C L}^{-1} \text{h}^{-1}$, with an average (SD) of 0.92 (0.46) $\mu\text{g C L}^{-1} \text{h}^{-1}$. These rates are more comparable with those observed in southern Québec aquatic ecosystems, and productive systems elsewhere, for example the high-nutrient Butron River, Vizcaya, Spain (Table 4). In this river, free-living bacteria had a production rate of $5.8 \mu\text{g C L}^{-1} \text{h}^{-1}$, with particle-attached communities contributing $2.97 \mu\text{g C L}^{-1} \text{h}^{-1}$ of bacterial-production (Iriberry et al., 1990).

Such comparisons with other sites need to be made with caution because they rest on a number of untested assumptions. Notably, we used a single factor for conversion between leucine uptake to carbon production concentrations, and assumed a 2-fold isotopic dilution of leucine in the natural environment, observed in certain subarctic ecosystems (Simon and Kirchman, 1988; Simon and Azam, 1989) and as has been employed for a wide range of bacterial production



540 studies elsewhere (Judd et al., 2006; del Giorgio et al., 1997; del Giorgio and Bouvier, 2002).
541 However, given the wide-range of DOC concentrations and unique characteristics of thermokarst
542 lakes, it is likely that the true conversion factors would lie on a wider range, as found in Pulido-
543 Villena and Reche (2003). If ambient leucine concentrations follow the trend of measured total
544 DOC concentrations, then production rates may have been especially underestimated in the SAS
545 incubations. This should not have influenced the pattern amongst size fractions, however, as
546 noted above, errors associated with cell counts for the particle-associated fractions may have
547 affected the estimates of rates per biomass.

548 The enrichment experiment in the present study showed that there was no significant
549 effect of either glucose or phosphorus when added separately. These results imply that bacterial
550 stocks and production were not strongly limited by carbon supply, nor were they subject to
551 primary phosphorus limitation. This contrasts with results from the permafrost-influenced, turbid
552 waters of the Mackenzie River, Northwest Territories Canada, where short-term glucose
553 enrichment resulted in a 4-fold increase in leucine uptake rates (Vallières et al., 2008). They also
554 contrast with enzymatic analyses of Greenland lakes that implied strong primary phosphorus
555 limitation. Chl *a* levels also showed no significant effect of enrichment, in contrast to such
556 experiments in High Arctic lakes (Bonilla et al., 2005). However, for the addition of glucose plus
557 phosphorus, and also for the soil addition treatment, there was a significant increase in specific
558 growth rates. This implies a combined stimulatory enrichment effect on bacterial production of
559 the palsa permafrost soils eroding into the SAS thermokarst lakes.

560 Other studies have shown that DOM-enrichment increased heterotrophic metabolism,
561 sometimes at the expense of autotrophic metabolic activity (Forsström et al., 2013). In an Arctic
562 tundra lake of the Northwest Territories, addition of permafrost soil resulted in decreased



563 bacterial production in the pelagic zone, but increased rates in the benthic zone (Moquin and
564 Wrona, 2015). A recent study of Arctic lakes in southwest Greenland found that microbial
565 populations were primarily phosphorus-limited, and that this P-limitation increased with the
566 availability of DOM (Burpee et al., 2016). In an area of discontinuous permafrost in northern
567 Sweden, addition of terrestrial carbon to aquatic bacterial samples resulted in a four- to seven-
568 fold increase in respiration rates, with only a small proportion of the available carbon (1 – 12%)
569 contributing to cellular biomass and the dominant portion respired to CO₂ (Roehm et al., 2009).

570 All of the limnological and microbial measurements point to the SAS peatland lakes as
571 favorable environments for bacterial production. The bacterial growth rates show that SAS lakes
572 were outliers amongst thermokarst lakes, with significantly elevated rates (Table 4). These rates
573 are also on the higher end of observations made across a wide trophic range of lakes from other
574 regions (del Girogio et al., 1997; Smith and Prairie, 2004). The lack of response of cellular rates
575 to either phosphorus or carbon added singly also implies sufficiency, and even although there
576 was a significant rise in growth in response to soil and carbon+phosphorus (G+P), this was not
577 translated into an increase in population size. In fact populations fell in all of the incubations,
578 despite bacterial community growth rates that remained the same or higher.. In combination,
579 these observations suggest that bacterial biomass in the SAS peatland lakes is controlled by top
580 down processes rather than by bottom-up, substrate supply rates. This might involve viral lysis,
581 as in planktonic bacterial systems elsewhere (e.g., Lymer et al., 2008) or it may be the result of
582 intense grazing by bacterivores. These waters contain high concentrations of zooplankton,
583 including *Daphnia* (Bégin 2014) that can filter picocyanobacteria (Przytulska et al., 2015) and
584 probably heterotrophic bacteria (Rautio and Vincent, 2006). Studies on SAS2A have shown that
585 they contain abundant ciliates, heterotrophic nanoflagellates and mixotrophic phytoplankton



586 (Przytulska et al., 2016), all of which may exert a control on bacterial densities. In these
587 environments, enriched by soil particles, carbon and nutrients released from thawing and eroding
588 permafrost, bacterial stocks may be ultimately capped by loss rather than gain processes.

589



590 **5 Acknowledgements**

591 This study was made possible with financial support from the Natural Sciences and Engineering
592 Research Council of Canada (NSERC), the Canada Research Chair program, and the Québec
593 nature and technology research funds (FRQNT). Financial and logistical support are further
594 provided by the Centre for Northern Studies (Université Laval), the ADAPT (Arctic
595 Development and Adaptation to Permafrost in Transition) Discovery Frontiers grant, and the
596 Northern Science Training Program. We thank P. Bégin, J. Comte, A. Przytulska-Bartosiewicz,
597 V. Mohit, and C. Tremblay for their help in the field, and M.-J. Martineau for laboratory support.
598 We thank D. Sarrazin and S. Aebischer for permafrost core sampling, and the CEN-ADAPT team
599 for core and CHN analysis: G. Labrecque, A.-S. Carbonneau, J. Roger and M. Lemay. We thank
600 S. Prémont at the INRS-ETE laboratory and D. Cayer at Université Laval FFGG laboratory for
601 support and guidance with sample analysis.

602



603 6 References

- 604 Acinas, S. G., Antón, J., and Rodríguez-Valera, F.: Diversity of free-living and attached bacteria
605 in offshore western Mediterranean waters as depicted by analysis of genes encoding 16S
606 rRNA, *Appl. Environ. Microbiol.*, 65, 514-522, 1999.
- 607 ADAPT: Carbon, nitrogen and water content of the active layer from sites across the Canadian
608 Arctic, v. 1.0, Nordicana D21, doi:10.5885/45327AD-5245D08606AB4F52, 2014.
- 609 Alldredge, A. L., and Silver, M. W.: Characteristics, dynamics and significance of marine snow,
610 *Progr. Oceanogr.*, 20, 41-82, 1988.
- 611 Amon, R. M. W., and Benner, R.: Bacterial utilization of different size classes of dissolved
612 organic matter, *Limnol. Oceanogr.*, 41, 41-51, 1996.
- 613 Arlen-Pouliot, Y., and Bhiry, N.: Palaeoecology of a palsa and a filled thermokarst pond in a
614 permafrost peatland, subarctic Québec, Canada, Holocene, 15, 408-419,
615 doi:10.1191/0959683605hl818rp, 2005.
- 616 Bégin, P.-N.: Abondance et diversité des rotifères dans les mares de thermokarst subarctiques,
617 M.Sc., Département de biologie, Université Laval, Canada, 2015.
- 618 Bhiry, N., Delwaide, A., Allard, M., Bégin, Y., Filion, L., Lavoie, M., Nozais, C., Payette, S.,
619 Pienitz, R., and Saulnier-Talbot, É.: Environmental change in the Great Whale River
620 region, Hudson Bay: Five decades of multidisciplinary research by Centre d'études
621 nordiques (CEN), *Ecoscience*, 18, 182-203, doi:10.2980/18-3-3469, 2011.
- 622 Bonilla, S., Villeneuve, V. and Vincent W. F.: Benthic and planktonic algal communities in a
623 high arctic lake: Pigment structure and contrasting responses to nutrient enrichment, *J.*
624 *Phycol.*, 41, 1120-1130, doi:10.1111/j.1529-8817.2005.00154.x, 2005.
- 625 Bowden, W. B., Gooseff, M. N., Balser, A., Green, A., Peterson, B. J., and Bradford, J.:
626 Sediment and nutrient delivery from thermokarst features in the foothills of the North
627 Slope, Alaska: Potential impacts on headwater stream ecosystems, *J. Geophys. Res.*, 113,
628 G02026, doi:10.1029/2007JG000470, 2008.
- 629 Bowen, H. J. M.: *Environmental Chemistry of the Elements*, Academic Press, London, UK,
630 1979.
- 631 Breton, J., Prairie, Y., Vallières, C., and Laurion, I.: Limnological properties of permafrost thaw
632 ponds in northeastern Canada, *Can. J. Fish. Aquat. Sci.*, 66, 1635-1648, doi:10.1139/f09-
633 108, 2009.
- 634 Burpee, B., Saros, J. E., Northington, R. M., and Simon, K. S.: Microbial nutrient limitation in
635 Arctic lakes in a permafrost landscape of southwest Greenland, *Biogeosciences*, 13, 365-
636 374, doi:10.5194/bg-13-365-2016, 2016.
- 637 Calmels, F., and Allard, M.: Ice segregation and gas distribution in permafrost using
638 tomodesitometric analysis, *Permafrost Periglac.*, 15, 367-378, doi:10.1002/ppp.508,
639 2004.
- 640 Calmels, F., Gagnon, O., and Allard, M.: A portable earth-drill system for permafrost studies,
641 *Permafrost Periglac.*, 16, doi:311-315, 10.1002/ppp.529, 2005.



- 642 Crevecoeur, S., Vincent, W. F., Comte, J., and Lovejoy, C.: Bacterial community structure across
643 environmental gradients in permafrost thaw ponds: methanotroph-rich ecosystems, *Front.*
644 *Microbiol.*, 6, 192, doi:10.3389/fmicb.2015.00192, 2015.
- 645 Crump, B. C., Armbrust, E. V., and Baross, J. A.: Phylogenetic analysis of particle-attached and
646 free-living bacterial communities in the Columbia River, its estuary, and the adjacent
647 coastal ocean, *Appl. Environ. Microbiol.*, 65, 3192-3204, 1999.
- 648 Crump, B. C., Baross, J. A., and Simenstad, C. A.: Dominance of particle-attached bacteria in the
649 Columbia River estuary, USA, *Aquat. Microb. Ecol.*, 14, 7-18, 1998.
- 650 del Giorgio, P. A., and Bouvier, T. C.: Linking the physiologic and phylogenetic successions in
651 free-living bacterial communities along an estuarine salinity gradient, *Limnol. Oceanogr.*,
652 47, 471-486, doi:10.4319/lo.2002.47.2.0471, 2002.
- 653 del Giorgio, P. A., Prairie, Y., and Bird, D. F.: Coupling between rates of bacterial production
654 and the abundance of metabolically active bacteria in lakes, enumerated using CTC
655 reduction and flow cytometry, *Microb. Ecol.*, 34, 144-154, doi:10.1007/s002489900044,
656 1997.
- 657 Deshpande, B. N., MacIntyre, S., Matveev, A., and Vincent, W. F.: Oxygen dynamics in
658 permafrost thaw lakes: Anaerobic bioreactors in the Canadian subarctic, *Limnol.*
659 *Oceanogr.*, 60, 1656-1670, doi:10.1002/lno.10126, 2015.
- 660 Fichot, C. G., and Benner, R.: The spectral slope coefficient of chromophoric dissolved organic
661 matter (S275-295) as a tracer of terrigenous dissolved organic carbon in river-influenced
662 ocean margins, *Limnol. Oceanogr.*, 57, 1452-1466, doi:10.4319/lo.2012.57.5.1453, 2012.
- 663 Fillion, M.-E., Bhiry, N., and Touazi, M. Differential development of two palsa fields in a
664 peatland located near Whapmagoostui-Kuujuarapik, Northern Quebec, Canada, *Arct.*
665 *Antarct. Alp. Res.*, 46, 40-54, doi:10.1657/1938-4246-46.1.40, 2014.
- 666 Fletcher, M.: The physiological activity of bacteria attached to solid surfaces, *Adv. Microb.*
667 *Physiol.*, 32, 53-85, 1990.
- 668 Forsström, L., Roiha, T., and Rautio, M.: Responses of microbial food web to increased
669 allochthonous DOM in an oligotrophic subarctic lake, *Aquat. Microb. Ecol.*, 68, 171-184,
670 2013.
- 671 Galand, P. E., Lovejoy, C., Pouliot, J., and Vincent, W. F.: Heterogeneous archaeal communities
672 in the particle-rich environment of an arctic shelf ecosystem, *J. Marine Syst.*, 74, 774-782,
673 doi:10.1016/j.jmarsys.2007.12.001, 2008.
- 674 Garneau, M.-È., Vincent, W. F., Alonso-Sáez, L., Gratton, Y., and Lovejoy, C.: Prokaryotic
675 community structure and heterotrophic production in a river-influenced coastal arctic
676 ecosystem, *Aquat. Microb. Ecol.*, 42, 27-40, doi:10.3354/ame042027, 2006.
- 677 Ghiglione, J. F., Mevel, G., Pujo-Pay, M., Mousseau, L., Lebaron, P., and Goutx, M.: Diel and
678 seasonal variations in abundance, activity, and community structure of particle-attached
679 and free-living bacteria in NW Mediterranean Sea, *Microb. Ecol.*, 54, 217-231, 2007.
- 680 Gorham, E., and Janssens, J. A.: The distribution and accumulation of chemical elements in five
681 peat cores from the mid-continent to the eastern coast of North America, *Wetlands*, 25,
682 259-278, 2005.



- 683 Gorham, E., Lehman, C., Dyke, A., Clymo, D., and Janssens, J., Long-term carbon sequestration
684 in North American peatlands, *Quat. Sci. Rev.*, 58, 77-82,
685 doi:10.1016/j.quascirev.2012.09.018, 2012.
- 686 Grossart, H. P., and Simon, M.: Limnetic macroscopic organic aggregates (lake snow):
687 Occurrence, characteristics, and microbial dynamics in Lake Constance, *Limnol.*
688 *Oceanogr.*, 38, 532-546, 1993.
- 689 Höfle, S., Rethemeyer, J., Mueller, C. W., and John, S.: Organic matter composition and
690 stabilization in a polygonal tundra soil of the Lena-Delta, *Biogeosciences*, 10, 3145-3158,
691 doi:10.5194/bg-10-3145-2013, 2013.
- 692 Iriberri, J., Unanue, M., Ayo, B., Barcina, I., and Egea, L.: Bacterial production and growth rate
693 estimation from [3H] thymidine incorporation for attached and free-living bacteria in
694 aquatic systems, *Appl. Environ. Microbiol.*, 56, 483-487, 1990.
- 695 Judd, K. E., Crump, B. C., and Kling, G. W.: Variation in dissolved organic matter controls
696 bacterial production and community composition, *Ecology*, 87, 2068-2079, 2006.
- 697 Kankaala, P., Huotari, J., Peltomaa, E., Saloranta, T., and Ojala, A. Methanotrophic activity in
698 relation to methane efflux and total heterotrophic bacterial production in a stratified,
699 humic, boreal lake, *Limnol. Oceanogr.*, 51, 1195-1204, doi:10.4319/lo.2006.51.2.1195,
700 2006.
- 701 Karlsson, J., Jonsson, A., and Jansson, M.: Bacterioplankton production in lakes along an altitude
702 gradient in the subarctic north of Sweden, *Microb. Ecol.*, 42, 372-382, 10.1007/s00248-
703 001-0009-9, 2001.
- 704 Kirchman, D. L., and Ducklow, H. W.: Trophic dynamics of particle-bound bacteria in pelagic
705 ecosystems: a review, in: Moriaty, D. J. W., and Pullin, R. S. V. (eds.) *Detritus and*
706 *Microbial Ecology in Aquaculture*, ICLARM Conference Proceedings 14, International
707 Center for Living Aquatic Resources Management, Manila, Philippines, 54-82, 1987.
- 708 Kirchman, D. L., Keel, R. G., Simon, M., and Welschmeyer, N. A.: Biomass and production of
709 heterotrophic bacterioplankton in the oceanic subarctic Pacific, *Deep Sea Res. Part 1*
710 *Oceanogr. Res. Pap.*, 40, 967-988, 1993.
- 711 Kirchman, D., and Mitchell, R.: Contribution of particle-bound bacteria to total
712 microheterotrophic activity in five ponds and two marshes, *Appl. Environ. Microbiol.*, 43,
713 200-209, 1982.
- 714 Kirchman, D.: Measuring bacterial biomass production and growth rates from leucine
715 incorporation in natural aquatic environments, *Methods Microbiol.*, 30, 227-237,
716 doi:10.1016/S0580-9517(01)30047-8, 2001.
- 717 Kling, G. W., Kipphut, G. W., and Miller, M. C.: Arctic lakes and streams as gas conduits to the
718 atmosphere: Implications for tundra carbon budgets, *Science*, 251, 298-301, 1991.
- 719 Lami, R., Cuperoa, Z., Ras, J., Lebaron, P., and Koblížek, M.: Distribution of free-living and
720 particle-attached aerobic anoxygenic phototrophic bacteria in marine environments,
721 *Aquat. Microb. Ecol.*, 55, 31-38, 2009.



- 722 Laurion, I., Vincent, W. F., Retamal, L., Dupont, C., Francus, P., MacIntyre, S., and Pienitz, R.:
723 Variability in greenhouse gas emissions from permafrost thaw ponds, *Limnol. Oceanogr.*,
724 55, 115-133, doi:10.4319/lo.2010.55.1.0115, 2010.
- 725 Liebner, S., Ganzert, L., Kiss, A., Yang, S., Wagner, D., and Svenning, M. M.: Shifts in
726 methanogenic community composition and methane fluxes along the degradation of
727 discontinuous permafrost, *Front. Microbiol.*, 6, 356, doi:10.3389/fmicb.2015.00356,
728 2015.
- 729 Lymer, D., Lindström, E. S. and Vrede, K.: Variable importance of viral-induced bacterial
730 mortality along gradients of trophic status and humic content in lakes, *Freshwater Biol.*,
731 53, 1101–1113, doi:10.1111/j.1365-2427.2008.02015.x, 2008.
- 732 Masin, M., Uperova, Z. C., Hojerova, E., Salka, I., Grossart, H.-P., and Koblizek, M.:
733 Distribution of aerobic anoxygenic phototrophic bacteria in glacial lakes of northern
734 Europe, *Aquat. Microb. Ecol.*, 66, 77-86, 2012.
- 735 McClelland, J. W., Stieglitz, M., Pan, F., Holmes, R. M., and Peterson, B. J.: Recent changes in
736 nitrate and dissolved organic carbon export from the upper Kuparuk River, North Slope,
737 Alaska, *J Geophys Res*, 112, G04S60, doi:10.1029/2006JG000371, 2007.
- 738 Michaels, A. F., and Silver, M. W.: Primary production, sinking fluxes and the microbial food
739 web, *Deep Sea Res. Part 1 Oceanogr. Res. Pap.*, 35, 473-490, 1988.
- 740 Moquin, P. A., and Wrona, F. J.: Effects of permafrost degradation on water and sediment quality
741 and heterotrophic bacterial production of Arctic tundra lakes: An experimental approach,
742 *Limnol. Oceanogr.*, 60, 1484–1497, doi:10.1002/lno.10110, 2015.
- 743 Ploug, H., and Grossart, H. P.: Bacterial growth and grazing on diatom aggregates: Respiratory
744 carbon turnover as a function of aggregate size and sinking velocity, *Limnol. Oceanogr.*,
745 45, 1467-1475, 2000.
- 746 Przytulska, A., Bartosiewicz, M., Rautio, M., Dufresne, F., and Vincent, W.F.: Climate effects on
747 Arctic *Daphnia* via food quality and thresholds, *PLoS ONE*, 10, e0126231,
748 doi:10.1371/journal.pone.0126231, 2015.
- 749 Przytulska, A., Comte, J., Crevecoeur, S., Lovejoy, C., Laurion, I., and Vincent, W. F.:
750 Phototrophic pigment diversity and picophytoplankton in permafrost thaw lakes,
751 *Biogeosciences*, 13, 13-26, doi:10.5194/bg-13-13-2016, 2016.
- 752 Pulido-Villena, E., and Reche, I.: Exploring bacterioplankton growth and protein synthesis to
753 determine conversion factors across a gradient of dissolved organic matter, *Microb Ecol*,
754 46, 33-42, doi:10.1007/s00248-002-0004-9, 2003.
- 755 Rautio, M., and Vincent, W. F.: Benthic and pelagic food resources for zooplankton in shallow
756 high-latitude lakes and ponds, *Freshwater Biol.*, 51, 1038-1052, doi:10.1111/j.1365-
757 2427.2006.01550.x, 2006.
- 758 Roehm, C. L., Giesler, R., and Karlsson, J.: Bioavailability of terrestrial organic carbon to lake
759 bacteria: The case of a degrading subarctic permafrost mire complex, *J. Geophys. Res.*,
760 114, G03006, doi:10.1029/2008JG000863, 2009.
- 761 Roiha, T., Laurion, I., and Rautio, M.: Carbon dynamics in highly heterotrophic subarctic thaw
762 ponds, *Biogeosciences*, 12, 7223-7237, doi:10.5194/bg-12-7223-2015, 2015.



- 763 Roiha, T., Tirola, M., Cazzanelli, M., and Rautio, M.: Carbon quantity defines productivity
764 while its quality defines community composition of bacterioplankton in subarctic ponds,
765 *Aquat. Sci.*, 74, 513-525, doi:10.1007/s00027-011-0244-1, 2012.
- 766 Rossi, P., Laurion, I., and Lovejoy, C.: Distribution and identity of bacteria in subarctic
767 permafrost thaw ponds, *Aquat. Microb. Ecol.*, 69, 231-245, doi:10.3354/ame01634, 2013.
- 768 Simon, M., Alldredge, A. L., and Azam, F.: Bacterial carbon dynamics on marine snow, *Mar.*
769 *Ecol. Prog. Ser.*, 65, 205-211, 1990.
- 770 Simon, M., and Azam, F.: Protein content and protein synthesis rates of planktonic marine
771 bacteria, *Mar. Ecol. Prog. Ser.*, 51, 201-213, 1989.
- 772 Simon, M., and Kirchman, D.: Isotope dilution during bacterial amino acid uptake in the
773 subarctic Pacific: evidence for ammonium utilization by bacteria, *EOS*, 69, 1146, 1988.
- 774 Smith, D. C., and Azam, F.: A simple, economical method for measuring bacterial protein
775 synthesis rates in seawater using 3H-leucine, *Mar. Microb. Food Webs*, 6, 107-114, 1992.
- 776 Smith, E. M., and Prairie, Y. T.: Bacterial metabolism and growth efficiency in lakes: The
777 importance of phosphorus availability, *Limnol. Oceanogr.*, 49, 137-147, 2004.
- 778 Tarnocai, C., Canadell, J. G., Schuur, E. A. G., Kuhry, P., Mazhitova, G., and Zimov, S.: Soil
779 organic carbon pools in the northern circumpolar permafrost region, *Global Biogeochem.*
780 *Cy.*, 23, GB2023, doi:10.1029/2008GB003327, 2009.
- 781 Tuolonen, T., Kankaala, P., Ojala, A., and Arvola, L.: Factors controlling production of
782 phytoplankton and bacterial under ice in a humic, boreal lake, *J. Plankton Res.*, 16, 1411-
783 1432, 1994.
- 784 Unanue, M., Ayo, B., Azúa, I., Barcina, I., and Iriberri, J.: Temporal variability of attached and
785 free-living bacteria in coastal waters, *Microb. Ecol.*, 23, 27-39, 1992.
- 786 Vallières, C., Retamal, L., Ramlal, P., Osburn, C. L., and Vincent, W. F.: Bacterial production
787 and microbial food web structure in a large arctic river and the coastal Arctic Ocean, *J.*
788 *Mar. Syst.*, 74, 756-773, doi:10.1016/j.jmarsys.2007.12.002, 2008.
- 789 Vonk, J. E., Tank, S. E., Bowden, W. B., Laurion, I., Vincent, W. F., Alekseychik, P., Amyot,
790 M., Billet, M. F., Canário, J., Cory, R. M., Deshpande, B. N., Helbig, M., Jammet, M.,
791 Karlsson, J., Larouche, J., MacMillan, G., Rautio, M., Walter Anthony, K. M., and
792 Wickland, K.P.: Effects of permafrost thaw on arctic aquatic ecosystems, *Biogeosciences*
793 12, 7129-7167, doi:10.5194/bg-12-7129-2015, 2015.
- 794 Waidner, L. A., and Kirchman, D. L.: Aerobic anoxygenic phototrophic bacteria attached to
795 particles in turbid waters of the Delaware and Chesapeake estuaries, *Appl. Environ.*
796 *Microbiol.*, 73, 3936-3944, 2007.
- 797 Watanabe, S., Laurion, I., Chokmani, K., Pienitz, R., and Vincent, W. F.: Optical diversity of
798 thaw ponds in discontinuous permafrost: A model system for water color analysis, *J.*
799 *Geophys. Res.*, 116, G02003, doi:10.1029/2010jg001380, 2011.
- 800 Yoon, W. B., and Rosson, R. A.: Improved method of enumeration of attached bacteria for study
801 of fluctuation in the abundance of attached and free-living bacteria in response to diel
802 variation in seawater turbidity, *Appl. Environ. Microbiol.*, 56, 595-600, 1990.
- 803



7 Tables

Table 1. Chemical properties of permafrost soil samples from the palsa surface at SAS1. Each value is the mean (standard deviation) of triplicates.

Major constituents	Mean elemental concentration (SD) (g kg ⁻¹ dry weight)	Minor constituents	Mean elemental concentration (SD) (mg kg ⁻¹ dry weight)
Mg	0.339 (0.189)	Cd	0.12 (0.04)
Na	0.344 (0.123)	Pb	0.93 (0.46)
K	0.369 (0.178)	Mo	1.03 (0.18)
P	0.545 (0.019)	Ni	5.3 (0.8)
Al	3.67 (0.60)	Cr	5.8 (0.5)
S	4.86 (0.52)	Zn	5.8 (0.5)
Ca	5.23 (3.4)	Cu	6.5 (1.1)
Fe	6.04 (1.6)	Mn	24.5 (12)
N	30.0 (2.6)	Ba	43.5 (10)
C	509 (10.9)		



808 Table 2. Analysis from duplicate permafrost cores taken from palsas at the SAS2 study site. Gas,
 809 ice, and sediment (Sed) proportions (%) are by volume. a_{CDOM} (m^{-1}) is the CDOM absorption at
 810 440 nm. Dissolved organic carbon (DOC, in $mg\ L^{-1}$), soluble reactive phosphorus (SRP, in $\mu g\ L^{-1}$)
 811 $^{-1}$), and nitrate-nitrogen (NO_3 , in $\mu g\ N\ L^{-1}$) concentrations are potential contributions from melted
 812 core ice. N/A* = sample was below detection limit.

Core	Depth (m)	Gas (%)	Ice (%)	Sed (%)	a_{CDOM}	DOC	SRP	NO_3
A	1.25	5	95	0	12.0	14.7	N/A*	42.1
	1.75	18	82	0	13.3	13.9	N/A*	36.5
	2.77	1	41	58	51.5	28.0	33.1	341
B	1.25	3	97	0	16.2	26.9	N/A*	62.2
	1.75	5	95	0	14.0	17.9	N/A*	63.1
	2.77	2	53	44	10.0	28.8	20.8	93.6

813



814 Table 3. Limnological properties of study sites. Zs, sample depth, soluble reactive phosphorus
 815 (SRP, in $\mu\text{g L}^{-1}$), total nitrogen (TN, in mg L^{-1}), dissolved organic carbon (DOC, in mg L^{-1}),
 816 Chlorophyll *a* (Chl *a*, in $\mu\text{g L}^{-1}$), total suspended solids (TSS, in mg L^{-1}); PSmax, maximum
 817 frequency of particle size distribution (μm). The S samples correspond to surface at 0 m, and the
 818 B samples correspond to the maximum depth of each lake.

Lake	Zs	SRP	TN	DOC	Chl <i>a</i>	TSS	PSmax
SAS1A	S	1.01	0.58	10.4	3.31	5.31	452
	B	5.48	1.76	13.4	4.13	33.0	200
SAS1B	S	1.44	0.70	14.7	3.44	7.43	592
	B	2.18	0.89	14.6	6.22	11.3	262
SAS2A	S	1.42	0.42	8.50	0.94	17.6	300
	B	1.17	0.40	9.00	3.34	4.56	200
SAS2B	S	1.12	0.61	12.8	1.54	6.00	344
	B	8.34	1.88	22.0	7.78	16.5	1338
SAS2C	S	1.03	0.59	11.0	2.24	4.62	229
	B	5.76	1.71	21.0	1.84	15.8	229
KWK12	S	0.41	0.41	6.30	1.12	6.52	592
	B	1.78	0.63	7.60	6.24	27.1	200
SEC	S	0.75	0.26	2.90	1.02	6.97	153
	B	1.56	0.35	3.90	1.58	61.6	175
BGR1	S	0.42	0.24	2.40	0.49	4.57	59
	B	2.06	0.51	3.20	13.4	34.7	59
BGR2	S	1.85	0.38	5.10	0.92	30.8	229
NAS1A	S	4.18	0.25	3.80	0.32	112	102
	B	3.25	0.23	3.30	0.07	163	102
NAS1H	S	1.80	0.24	4.00	1.51	10.9	102
RBL4K	S	0.47	0.74	8.10	1.48	4.00	4
POND9K	S	4.84	0.81	15.1	1.16	3.22	13
RBL9K	S	3.66	0.54	10.2	0.88	1.28	200
RBLOlsha	S	1.09	0.36	9.10	2.05	1.46	175

819



820 Table 4. Bacterial properties of study sites. Zs, sample depth, bacterial abundance (BA, in 10^6
 821 cells mL^{-1} , bacterial production rate (BP, in $\mu\text{g C L}^{-1} \text{h}^{-1}$), and bacterial community specific
 822 growth rates (BG, in d^{-1}). The S samples correspond to surface at 0 m, and the B samples
 823 correspond to the maximum depth of each lake.

Lake	Zs	BA	BP	BG
SAS1A	S	0.319	0.896	3.72
	B	2.59	1.074	0.550
SAS1B	S	0.203	0.855	5.58
	B	0.867	0.923	1.41
SAS2A	S	3.15	0.254	0.107
	B	1.57	1.676	1.42
SAS2B	S	0.321	0.804	3.32
	B	1.26	0.588	0.619
SAS2C	S	0.282	1.34	6.30
	B	1.99	0.547	0.364
KWK12	S	3.53	2.34	0.879
	B	1.55	1.164	0.996
SEC	S	1.98	0.885	0.593
	B	0.994	0.650	0.867
BGR1	S	2.79	0.264	0.125
	B	1.03	0.609	0.784
BGR2	S	1.89	1.312	0.920
NAS1A	S	1.71	1.188	0.921
	B	1.16	0.785	0.897
NAS1H	S	0.864	1.253	1.92
RBL4K	S	2.46	0.371	0.200
POND9K	S	2.64	0.791	0.397
RBL9K	S	2.78	0.597	0.285
RBLOlsha	S	0.819	0.849	1.37

824



825 Table 5. Comparison of bacterial abundances (BA, 10^6 cells mL^{-1}) and production rates (BP, μg
 826 $\text{C L}^{-1} \text{h}^{-1}$) from thermokarst lakes with other aquatic environments. * Trophic status based on Chl
 827 a concentrations only.

Name	Location	Trophic status	BA	BP	Reference
Pääjärvi	Finland, in winter	Dystrophic	1.2 - 1.7	0.0083 - 0.096	Tulonen et al., 1994
16 ponds	Subarctic Finland	Oligotrophic	1.75 - 2.75	0.063 - 0.15	Roiha et al., 2012
Mesocosm of small tundra lake	Mackenzie Delta, Northwest Territories	Mesotrophic	--	0.16	Moquin and Wrona, 2015
SAS2A	Subarctic Québec	Dystrophic, mesotrophic	3.1	0.25	This study
BGR1	Subarctic Québec	Oligotrophic	2.8	0.26	This study
Stukely	Southern Québec	Mesotrophic*	2.7	0.30	del Giorgio et al., 1997
16 lakes	Subarctic Sweden	Oligotrophic, dystrophic	2.4 - 0.4	0.012 - 0.32	Karlsson et al., 2001
RBL4K	Subarctic Québec	Oligotrophic	2.5	0.37	This study
SEC	Subarctic Québec	Oligotrophic, mesotrophic	2.0	0.88	This study
SAS1A	Subarctic Québec	Dystrophic, mesotrophic	0.32	0.90	This study
NAS1A	Subarctic Québec	Oligotrophic, dystrophic	1.7	1.2	This study
SAS2C	Subarctic Québec	Dystrophic, mesotrophic	0.28	1.3	This study
Lovering	Southern Québec	Oligotrophic*	3.4	1.35	del Giorgio et al., 1997
Massawippi	Southern Québec	Mesotrophic*	3.0	1.69	del Giorgio et al., 1997
Magog	Southern Québec	Eutrophic*	3.38	1.88	del Giorgio et al., 1997
Central	Southern Québec	Mesotrophic*	3.3	2.15	del Giorgio et al., 1997
Brome	Southern Québec	Eutrophic*	3.4	2.24	del Giorgio et al., 1997
KWK12	Subarctic Québec	Mesotrophic, dystrophic	3.5	2.34	This study



828

Waterloo	Southern Québec	Hypereutrophic*	5.9	3.81	del Giorgio et al., 1997
----------	--------------------	-----------------	-----	------	-----------------------------



829 **8 Figure captions**

830 Figure 1. Map of the study regions and photos of the 6 study areas.

831 Figure 2. Palsas and their associated thermokarst lakes in the SAS valley. Upper panel: aerial
 832 view of the SAS1 area; lower panel ground-level view of SAS1B (photograph by Alexander
 833 Culley).

834 Figure 3. Percent carbon and nitrogen by dry weight in two permafrost cores from SAS palsa
 835 mounds, and proportions of gas, ice, and sediment by volume.

836 Figure 4. CDOM absorbance curve in SAS permafrost soil and lake water.

837 Figure 5. Distribution of particle sizes in lake water and permafrost soil samples. Insert in the top
 838 panel shows the soil sample particle-size distribution for both SAS valleys. The insert in the
 839 middle panel shows the particle-size distribution in three SAS lakes: SAS1A, SAS1B, and
 840 SAS2A. The bottom panel shows the particle-size distributions from the SAS2 permafrost core
 841 samples.

842 Figure 6. Difference spectra between the frequency distribution of particles in surface lake water
 843 (SAS2A) relative to active layer soil, permafrost and bottom lake water.

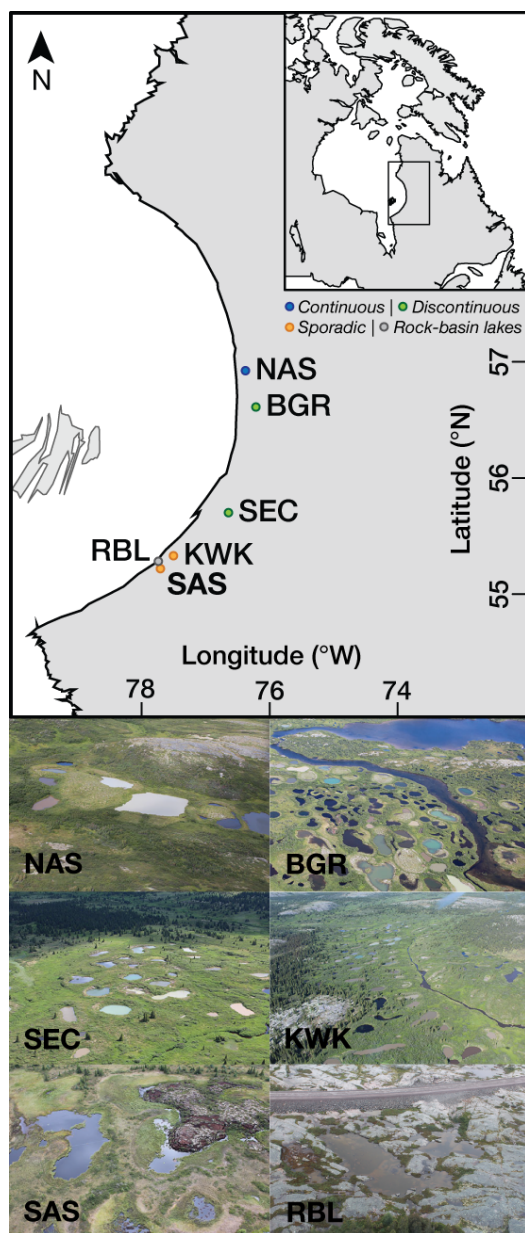
844 Figure 7. Size-fractionated total suspended solids (TSS), bacterial abundance (BA), bacterial
 845 production (BP), and bacterial cell-specific growth rates (BG) from five thermokarst lakes and
 846 one rock-basin lake. Each is the mean \pm SD of triplicate samples.

847 Figure 8. Planktonic variables in the 5-day experiment with amendments of phosphorus (P),
 848 glucose (G), glucose plus phosphorus (G+P), and palsa soil (S) to SAS1B lake water. The control
 849 (C) is shown on both day 1 and day 5. Each value is the mean \pm SD of triplicate samples.

850



851 Figure 1. Map of the study regions and photos of the 6 study areas.



852

853



854 Figure 2. Palsas and their associated thermokarst lakes in the SAS valley. Upper panel: aerial
855 view of the SAS1 area; lower panel ground-level view of SAS1B (photograph by Alexander
856 Culley).



857
858



Figure 3. Percent carbon and nitrogen by dry weight in two permafrost cores from SAS palsa
 mounds, and proportions of gas, ice, and sediment by volume.

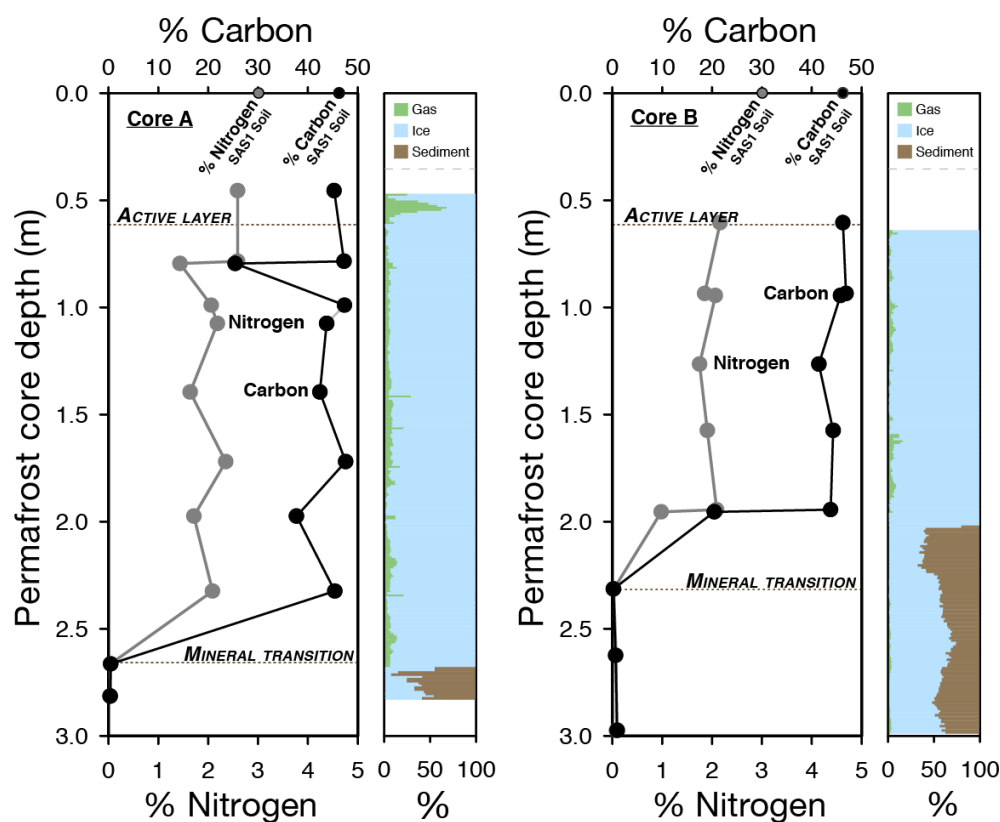




Figure 4. CDOM absorbance curve in SAS permafrost soil and lake water.

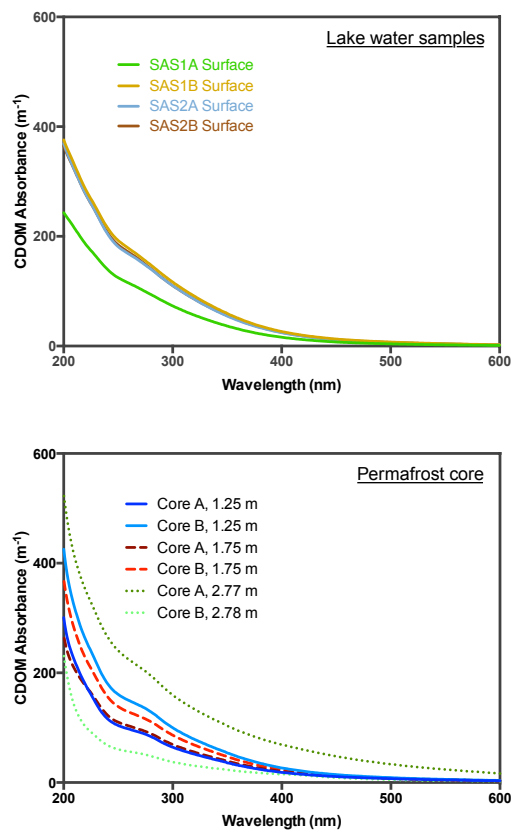
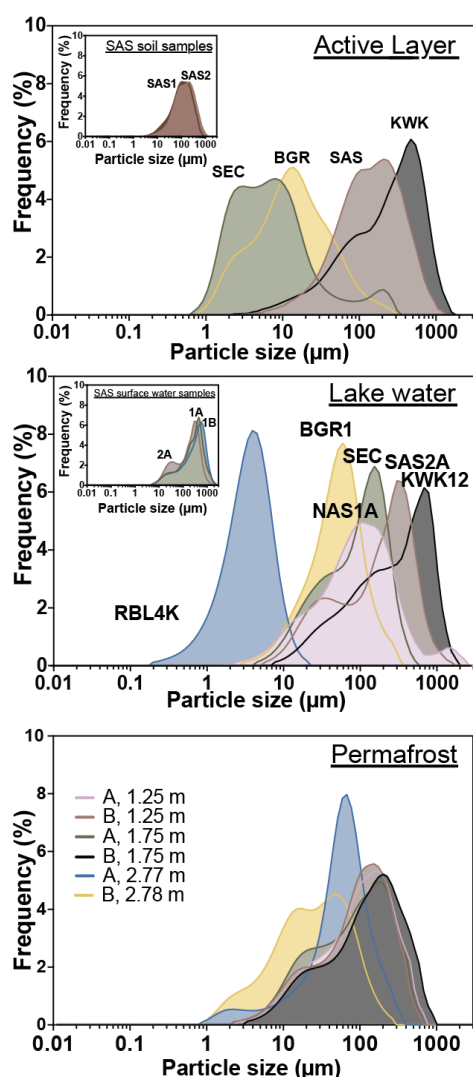


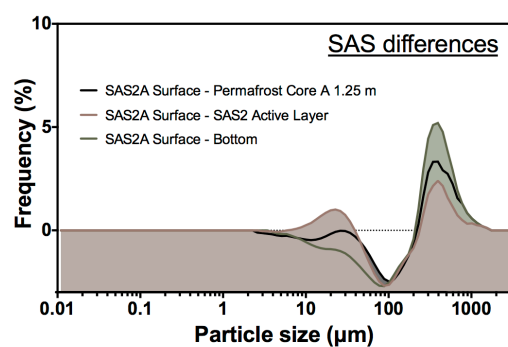


Figure 5. Distribution of particle sizes in lake water and permafrost soil samples. Insert in the top panel shows the soil sample particle-size distribution for both SAS valleys. The insert in the middle panel shows the particle-size distribution in three SAS lakes: SAS1A, SAS1B, and SAS2A. The bottom panel shows the particle-size distributions from the SAS2 permafrost core samples.





873 Figure 6. Difference spectra between the frequency distribution of particles in surface lake water
 874 (SAS2A) relative to active layer soil, permafrost and bottom lake water.



875
 876



Figure 7. Size-fractionated total suspended solids (TSS), bacterial abundance (BA), bacterial production (BP), and bacterial cell-specific growth rates (BG) from five thermokarst lakes and one rock-basin lake. Each is the mean \pm SD of triplicate samples.

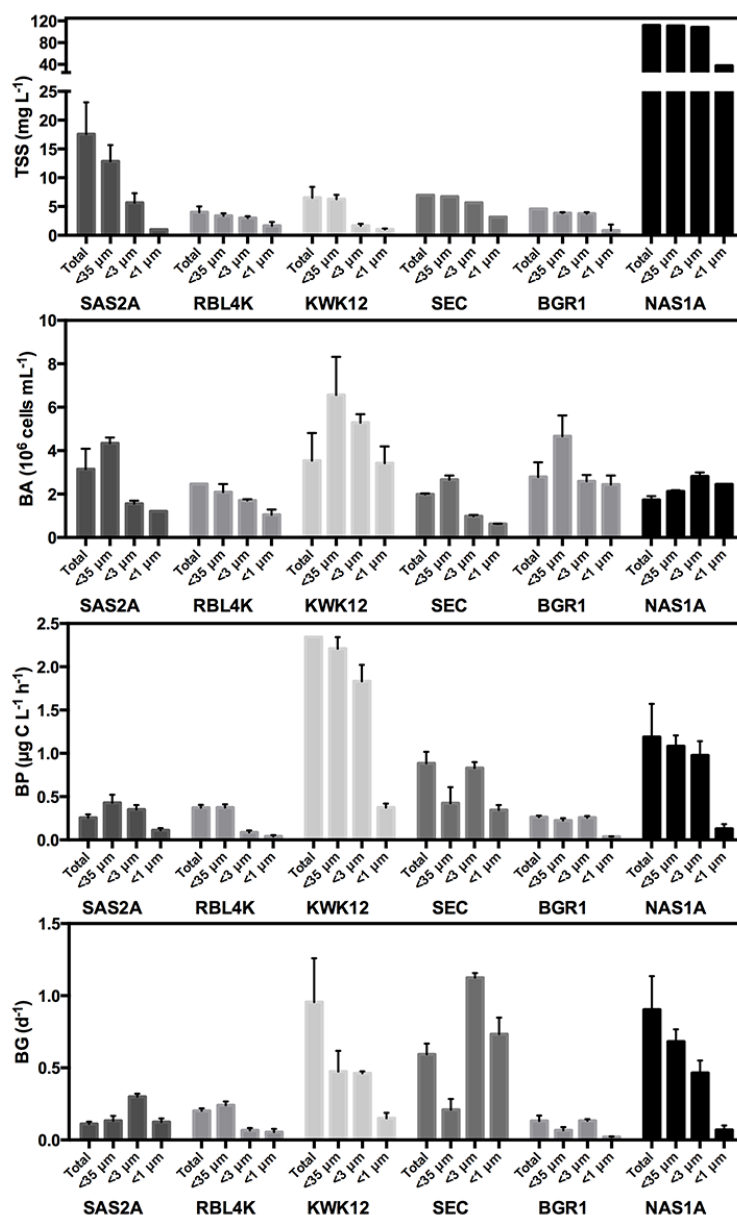




Figure 8. Planktonic variables in the 5-day experiment with amendments of phosphorus (P), glucose (G), glucose plus phosphorus (G+P), and palsa soil (S) to SAS1B lake water. The control (C) is shown on both day 1 and day 5. Each value is the mean \pm SD of triplicate samples.

